Insights into the Role of the Peroxisomal Ubiquitination Machinery in Pex13p Degradation in the Yeast Hansenula polymorpha

Chen, Xin; Devarajan, Srishti; Danda, Natasha; Williams, Chris

Published in:
Journal of Molecular Biology

DOI:
10.1016/j.jmb.2018.03.033

Publication date:
2018

Featured Article

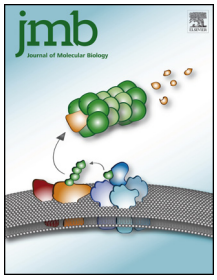

Insights into the Role of the Peroxisomal Ubiquitination Machinery in Pex13p Degradation in the Yeast *Hansenula polymorpha*

Xin Chen, Srishti Devarajan, Natasha Danda and Chris Williams

Molecular Cell Biology, *Groningen Biomolecular Sciences and Biotechnology Institute, University of Groningen, 9747AG Groningen, the Netherlands*

Correspondence to Chris Williams: *c.p.williams@rug.nl*
https://doi.org/10.1016/j.jmb.2018.03.033
Edited by M.F. Summers

Xin Chen, Srishti Devarajan, Natasha Danda and Chris Williams

Abstract

The import of matrix proteins into peroxisomes in yeast requires the action of the ubiquitin-conjugating enzyme Pex4p and a complex consisting of the ubiquitin E3 ligases Pex2p, Pex10p and Pex12p. Together, this peroxisomal ubiquitination machinery is thought to ubiquitinate the cycling receptor protein Pex5p and members of the Pex20p family of co-receptors, a modification that is required for receptor recycling. However, recent reports have demonstrated that this machinery plays a role in additional peroxisome-associated processes. Hence, our understanding of the function of these proteins in peroxisome biology is still incomplete. Here, we identify a role for the peroxisomal ubiquitination machinery in the degradation of the peroxisomal membrane protein Pex13p. Our data demonstrate that Pex13p levels build up in cells lacking members of this machinery and also establish that Pex13p undergoes rapid degradation in wild-type cells. Furthermore, we show that Pex13p is ubiquitinated in wild-type cells and also establish that Pex13p ubiquitination is reduced in cells lacking a functional peroxisomal E3 ligase complex. Finally, deletion of PEX2 causes Pex13p to build up at the peroxisomal membrane. Taken together, our data provide further evidence that the role of the peroxisomal ubiquitination machinery in peroxisome biology goes much deeper than receptor recycling alone.

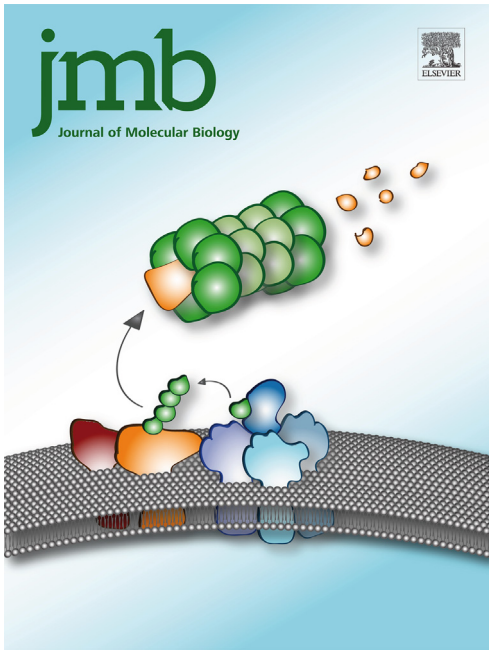

While pathways that target ER and mitochondrial membrane proteins for degradation are well studied, little is known about how peroxisomal membrane proteins are degraded. The manuscript of Chen *et al.* provides insights into how the peroxisomal membrane protein Pex13p is degraded in the yeast *Hansenula polymorpha*. The cover illustration depicts an artistic representation of Pex13p (orange) degradation by the ubiquitin–proteasome system (in green), showing the roles the E2 enzyme Pex4p (dark blue) and the E3 ligases Pex2p, Pex10p and Pex12p (light blue and purple) may play. Artwork by Chris Williams

Introduction

Peroxisomes are highly versatile eukaryotic organelles that play a vital role in regulating cellular metabolism, providing compartments where metabolic pathways can be contained and controlled. Their versatility is demonstrated by the wide range of metabolic pathways contained in peroxisomes. Some well-known peroxisomal processes include the oxidation of fatty acids and the biosynthesis of plasmalogens and penicillin, but many more exist [1]. Their importance in cell vitality is underscored by a number of inherited developmental brain disorders caused by defects in peroxisome biogenesis [2]. Peroxisomes require protein import systems to obtain both peroxisomal membrane (PMP) and matrix proteins, via the use of peroxisomal targeting signals (PTS) in the cargo protein. The mechanisms of PMP import are not well understood, although important roles for the PMP Pex3p and the cytosolic receptor protein Pex19p have been demonstrated [3,4]. In contrast, our understanding of the mechanisms that underlie matrix protein import is much more developed [5]. Matrix proteins containing a C-terminal PTS1 can be recognized by the cytosolic receptor Pex5p, while matrix proteins with an N-terminal PTS2 are recognized by Pex7p [6,7]. In yeasts, Pex7p requires members of the Pex20p family of co-receptor proteins to facilitate import, whereas this function is fulfilled by an isoform of Pex5p in higher eukaryotes [8]. Pex5p shuttles between the cytosol and peroxisomal membrane during the transport of PTS1-cargo proteins. The cargo-Pex5p complex, which forms in the cytosol, travels to the peroxisomal membrane, where it contacts the docking complex consisting of the PMPs Pex13p and Pex14p. After translocation of the cargo to the peroxisomal matrix in a process involving Pex8p, Pex5p is ubiquitinated, which facilitates its removal from the peroxisomal membrane (for a review on matrix protein import, see Ref. [5]).

Ubiquitination is a posttranslational modification that requires the activity of a three-step enzyme cascade [9]. The ubiquitin-activating enzyme (E1) activates the small protein ubiquitin (Ub) via ATP hydrolysis and transfers it to the active site cysteine of an ubiquitin-conjugation enzyme (E2). The final step requires the activity of an ubiquitin ligase (E3). Two classes of E3s exist. Members of the HECT class, much like E2s, accept Ub onto an active site cysteine and then transfer Ub to a substrate, whereas RING E3 ligases act as bridge between E2 and substrate, positioning the E2 active site in close proximity to the modification site in the substrate, allowing Ub transfer to occur.

Two distinct types of Pex5p ubiquitination have been reported. Mono-ubiquitination of Pex5p on a conserved cysteine residue in its N-terminal region by the E2 Pex4p allows Pex5p to recycle to the cytosol, ready to take part in another import round [10–12]. Poly-ubiquitination of Pex5p on lysine residues by the E2 Ubc4p, on the other hand, targets Pex5p for degradation via the proteasome [13,14]. For both types of Pex5p ubiquitination, a complex consisting of three peroxisomal RING E3s (Pex2p, Pex10p and Pex12p) is required [15,16], while extraction of ubiquitinated Pex5p from the membrane depends on a complex of the AAA-ATPase proteins Pex1p and Pex6p [17]. Pex20p family members can also undergo ubiquitination, either for recycling or for degradation, in a similar fashion to that mentioned for Pex5p [18].

It is evident that the peroxisomal ubiquitination machinery (Pex4p, Pex2p, Pex10p and Pex12p) is important for peroxisome function because of its role in receptor ubiquitination. However, recent reports link this machinery to the ubiquitination and/or degradation of additional peroxisomal proteins. For example, the PMP Pex3p from the yeast *Hansenula polymorpha* is ubiquitinated and degraded by the proteasome when cells are shifted from methanol to glucose containing media [19]. Pex3p degradation, which is inhibited in *pex2Δ* and *pex10Δ* cells, initiates the autophagic degradation of peroxisomes via pexophagy [20]. Pex2p is implicated in PMP70 ubiquitination in mammalian cells, which is also linked to pexophagy [21], while Pex4p is involved in the degradation of the PTS2 co-receptor protein Pex18p in *Saccharomyces cerevisiae* [22]. These reports demonstrate that the list of substrates targeted by the peroxisomal ubiquitination machinery is likely to be far from complete.

In this manuscript, we have investigated the role of the peroxisomal ubiquitination machinery in the degradation of the PMP Pex13p. Cells deleted for components of the peroxisomal ubiquitination machinery display enhanced Pex13p levels, while we also demonstrate that Pex13p is degraded in wild-type (WT) cells. Furthermore, we show that Pex13p is ubiquitinated in WT cells and that Pex13p ubiquitination is inhibited in cells lacking a functional peroxisomal E3 ligase complex. Finally, we demonstrate that deletion of *PEX2* causes Pex13p to build up on the peroxisomal membrane. Taken together, our data provide further evidence to support the suggestion that the role of the peroxisomal ubiquitination machinery goes much deeper than receptor ubiquitination alone.

Results

Pex13p levels are increased in cells deleted for components of the peroxisome ubiquitination machinery

While a role for the peroxisome ubiquitination machinery in receptor ubiquitination is well established, recent reports strongly suggest that this machinery

targets additional peroxisomal proteins. Therefore, we set out to identify potential new substrates of this machinery in the yeast *H. polymorpha* and were particularly interested in which PMPs may be targeted, since little is known about PMP degradation [23].

We reasoned that PMPs targeted for degradation by the peroxisomal ubiquitination machinery may display increased levels in cells deleted for components of this machinery. Therefore, we assessed the levels of a selection of PMPs in cells deleted for PEX2, PEX4, PEX10 or PEX12 grown on methanol/glycerol containing media. Methanol induces peroxisome proliferation, but because cells deleted for PEX genes generally cannot utilize methanol as carbon source and hence cannot grow on methanol, glycerol is added to the medium to support growth. The PMPs tested, which are involved in different peroxisomal functions, included Pex13p and Pex14p (both involved in matrix protein import [24,25]), Pex3p (involved in PMP import [26]) and Pex11p (involved in peroxisomal fission [27]). We observed that Pex13p levels were increased in all the tested strains compared to WT cells (Fig. 1a) and Pex13p levels appeared particularly enhanced in cells deleted for PEX2, PEX10 or PEX12. Similarly, cells expressing the K48R mutant form of Ub also displayed enhanced Pex13p levels, although not to the same extent as those deleted for one of the peroxisomal E3 ligases (Fig. 1a). Ub-K48R inhibits proteasomal-mediated degradation by blocking Ub chain formation on substrates [28], suggesting a link between Pex13p levels and the ubiquitin–proteasome system (UPS). A slight increase in Pex3p and Pex14p levels in these deletion strains was also observed (Fig. 1a). A role for the peroxisomal ubiquitination machinery in Pex3p degradation has already been proposed [19], although Pex3p degradation was shown to occur under different growth conditions from those used here. Pex11p levels appeared largely unaffected in the deletion strains (Fig. 1a).

To gain insight into the extent to which Pex13p levels were increased in these deletion strains compared to WT cells, we performed quantitative Western blotting, assessing the fold increase in Pex13p levels in *pex4Δ* and *pex2Δ* cells (Fig. 1b). Deletion of either PEX2, PEX10 or PEX12 results in inactivation of the entire E3 ligase complex [29], hence our choice to assess Pex13p levels in *pex2Δ* cells only. Pex13p levels increased around 4-fold in *pex4Δ* cells and around 12-fold in *pex2Δ* cells compared to WT. Quantification of our Western blots also confirmed that Pex14p levels were slightly increased in *pex2Δ* or *pex4Δ* cells compared to WT cells, although to a much lower extent than for Pex13p (Fig. 1b). As already suggested by Fig. 1a, Pex11p levels were not significantly affected by deletion of PEX2 or PEX4 (Fig. 1b). Because of the dramatic effect on Pex13p levels caused by these deletions, we chose to investigate Pex13p further.

Deletion of PEX2, PEX4, PEX10 or PEX12 inhibits the import of matrix proteins into peroxisomes [5]. Since the oxidation of methanol occurs inside peroxisomes and targeting the enzymes required for methanol utilization to the cytosol inhibits cells in their ability to grow on methanol, strains where matrix protein import is inhibited cannot utilize methanol as carbon source [30]. Therefore, we investigated whether the increased Pex13p levels in our deletion strains stem from an inability of these strains to utilize methanol. We compared the levels of Pex13p in WT cells against cells deleted for alcohol oxidase (AOX). AOX is required for methanol oxidation and cells deleted for AOX cannot utilize methanol [31]. We observed no increase in Pex13p levels in *aoxΔ* cells grown on methanol/glycerol containing media (Fig. 1c), indicating that the increased Pex13p levels in cells deleted for PEX2, PEX4, PEX10 or PEX12 are not caused by an inability of these cells to utilize methanol.

Next, to verify that the increased levels of Pex13p in these mutant strains were not a result of increased Pex13p expression, we placed mGFP under control of the PEX13 promoter and assessed mGFP levels in our deletion and Ub-K48R mutant strains. The level of mGFP in all mutants was comparable to that in WT cells (Fig. 1d). These data demonstrate that PEX13 expression is not up-regulated in these strains.

The major protein degradation pathway in eukaryotic cells is the UPS [32]. However, certain proteins can be degraded via autophagy [33], and although these two pathways are separate entities, crosstalk between the two pathways is well established [34]. For example, ubiquitination of PMP70 by Pex2p initiates pexophagy in mammalian cells [21], while we previously demonstrated that Pex10p plays a role in degradation of Pex3p, which in turn initiates pexophagy in *H. polymorpha* [19]. Hence, we considered the possibility that the effect on Pex13p levels in our deletion strains may result as a consequence of disturbances to pexophagy. To investigate this, we assessed the levels of Pex13p in an *atg1Δ* strain, in which pexophagy is inhibited [35]. We did not observe an increase in Pex13p levels in *atg1Δ* cells (Fig. 1e), demonstrating that increased Pex13p levels do not stem from inhibiting pexophagy but rather from a block in UPS-dependent degradation. Together, our data suggest that Pex13p is a potential substrate of the peroxisomal ubiquitination machinery.

Pex13p is degraded in WT cells and Pex13p degradation requires a functional peroxisomal E3 ligase complex

Since deleting components of the peroxisomal ubiquitination machinery seems to block Pex13p degradation (Fig. 1), our next step was to investigate whether Pex13p is actively degraded in WT cells. To achieve this, we assessed the stability of Pex13p in

WT cells treated with the protein synthesis inhibitor cycloheximide (CHX). We observed rapid decrease of Pex13p levels after CHX treatment (Fig. 2a and b), while similar behavior was evident with Pex13-mGFP (Fig. 2c and d), establishing that Pex13p is actively degraded in WT cells. We employed Pex13-mGFP because this also gave us the opportunity to investigate Pex13p localization using fluorescence microscopy (see below). In contrast, Pex13-mGFP turnover was reduced in cells expressing Ub-K48R

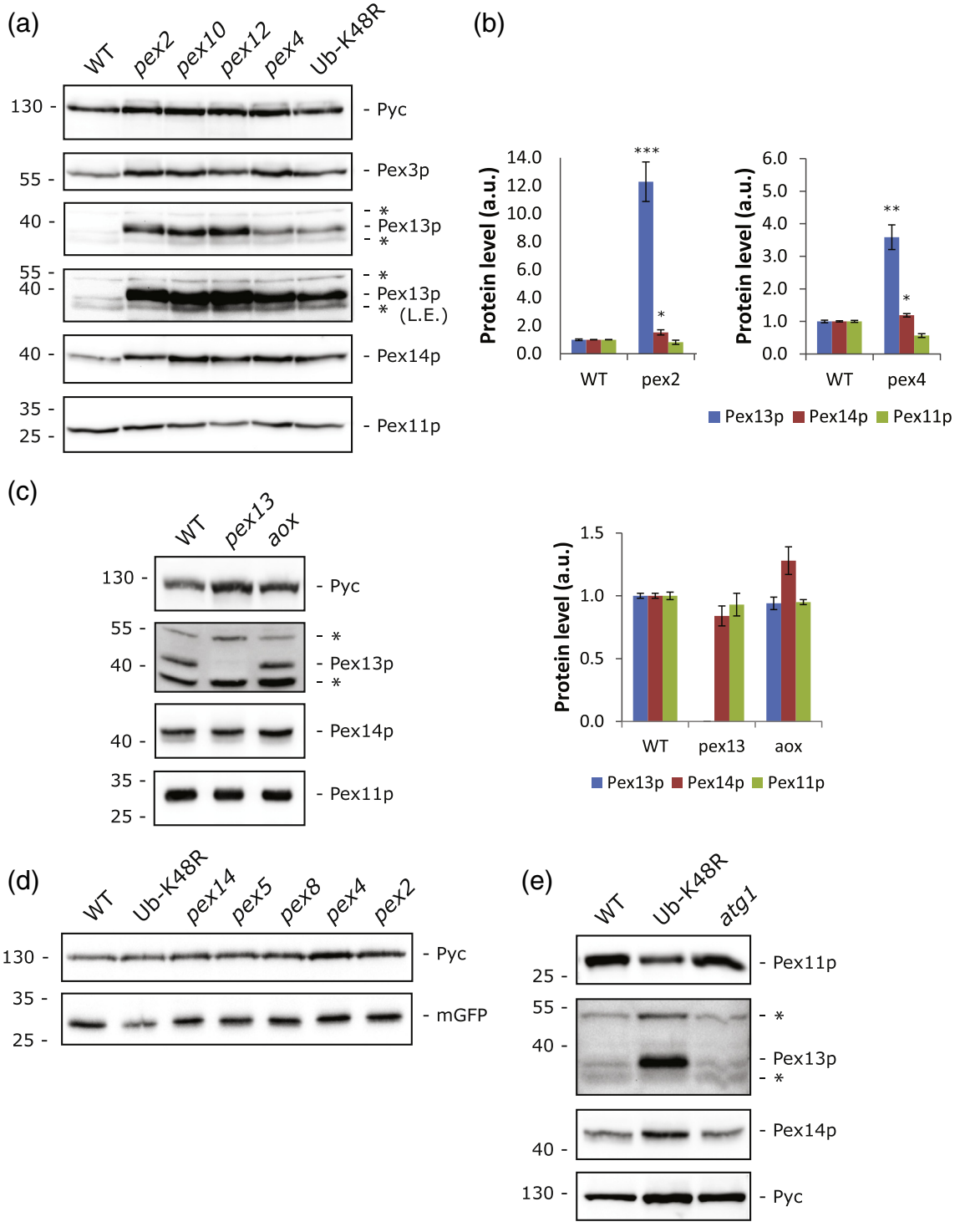

Fig. 1 (*legend on next page*)

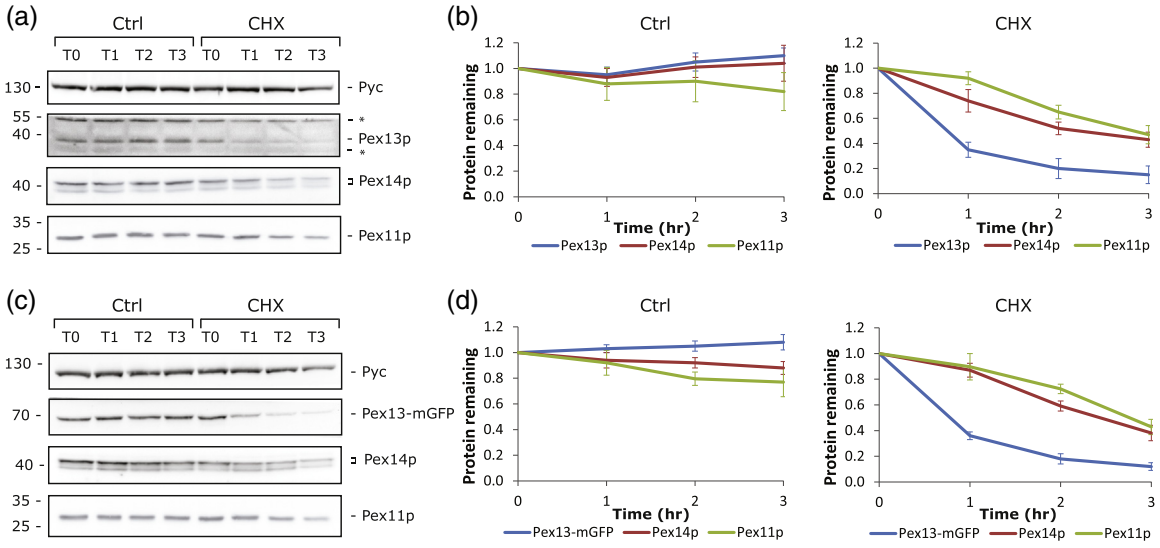

Fig. 2. *H. polymorpha* Pex13p is actively degraded in WT cells. (a) WT cells were grown on methanol/glycerol media for 12 h and then treated with DMSO (Ctrl) or CHX. TCA samples were taken at the indicated time (h) after DMSO/CHX addition and probed by SDS-PAGE and immunoblotting with antibodies against Pex13p, Pex14p, Pex11p and Pyc. * Denotes anti-Pex13p cross reactive species. (b) Quantification of Pex13p, Pex14p and Pex11p levels in WT cells treated with DMSO (Ctrl) or CHX. Protein levels were normalized to Pyc. Protein levels at T0 were set to 1. Values represent the mean ± SD of three independent experiments. (c) Representative Western blots of WT cells expressing Pex13-mGFP grown and treated as in panel a. Western blots were probed using antibodies against Pex14p, Pex11p, Pyc and mGFP. (d) Quantification of protein levels in WT cells expressing Pex13-mGFP after DMSO/CHX addition. The data were generated as in panel b. The blots used to quantify protein levels for panels b and d can be found in Figure S2.

(Fig. 3a and b) and in cells deleted for PEX2 (Fig. 3c and d), supporting our suggestion that Pex13p degradation is inhibited in cells lacking a functional peroxisomal E3 ligase complex, as well as in cells expressing Ub-K48R (Fig. 1).

We observed that the levels of Pex14p and Pex11p in our CHX experiments decreased over time, although at a lower rate than Pex13p (Fig. 2a–d). Also, Pex11p and Pex14p appeared stable in cells expressing Ub-K48R (Fig. 3a and b) and in *pex2Δ* cells (Fig. 3c and d). One possible way to interpret these data is that both Pex11p and Pex14p may also be degraded in a process that requires the peroxisomal E3 ligase complex and Ub, although further study will be required to determine whether this is indeed the case. Nevertheless, our data strongly suggest that Pex13p is actively degraded in a process that requires Ub and the peroxisomal E3 ligase complex.

Fig. 1. *H. polymorpha* Pex13p levels are elevated in cells deleted for components of the peroxisomal ubiquitination machinery. (a) WT cells, together with *pex2Δ*, *pex10Δ*, *pex12Δ* and *pex4Δ* cells and WT cells producing Ub-K48R grown for 16 h on methanol/glycerol media, were lysed and samples were subjected to SDS-PAGE and immunoblotting using antibodies directed against Pex3p, Pex13p, Pex14p, Pex11p and Pyc. * Denotes anti-Pex13p cross reactive species. L.E. stands for longer exposure. (b) Bar chart displaying Pex13p, Pex14p and Pex11p levels in WT, *pex2Δ* and *pex4Δ* cells. Values were derived from quantifying Western blots of samples prepared as in panel a. Protein levels were normalized to Pyc (loading control) and plotted against the levels in WT cells (set to 1). Values represent the mean ± SD of three independent experiments. Asterisks denote statistically significant increases in protein levels compared to those in WT samples (*$P < 0.05$, **$P < 0.01$, ***$P < 0.001$). (c) Representative Western blots of Pex13p, Pex14p, Pex11p and Pyc levels in WT, *pex13Δ* and *aoxΔ* cells grown and treated as in panel a. * Denotes anti-Pex13p cross reactive species. The right panel displays the quantification of Pex13p, Pex14p and Pex11p levels, normalized to the loading control Pyc. Protein levels in WT cells were set to 1. Values represent the mean ± SD of three independent experiments. (d) WT and mutant cells expressing mGFP under control of the PEX13 promoter (P_{PEX13}) were grown for 16 h on methanol/glycerol containing media and lysed, and samples were probed with SDS-PAGE and immunoblotting using antibodies against mGFP and Pyc. (e) TCA lysates of WT cells, WT cells producing Ub-K48R and *atg1Δ* cells grown on methanol/glycerol media for 16 h were subjected to SDS-PAGE, immunoblotting and probed with antibodies directed against Pex11p, Pex13p, Pex14p and Pyc. * Denotes anti-Pex13p cross reactive species. The blots used to quantify protein levels for panels b and c can be found in Figure S1.

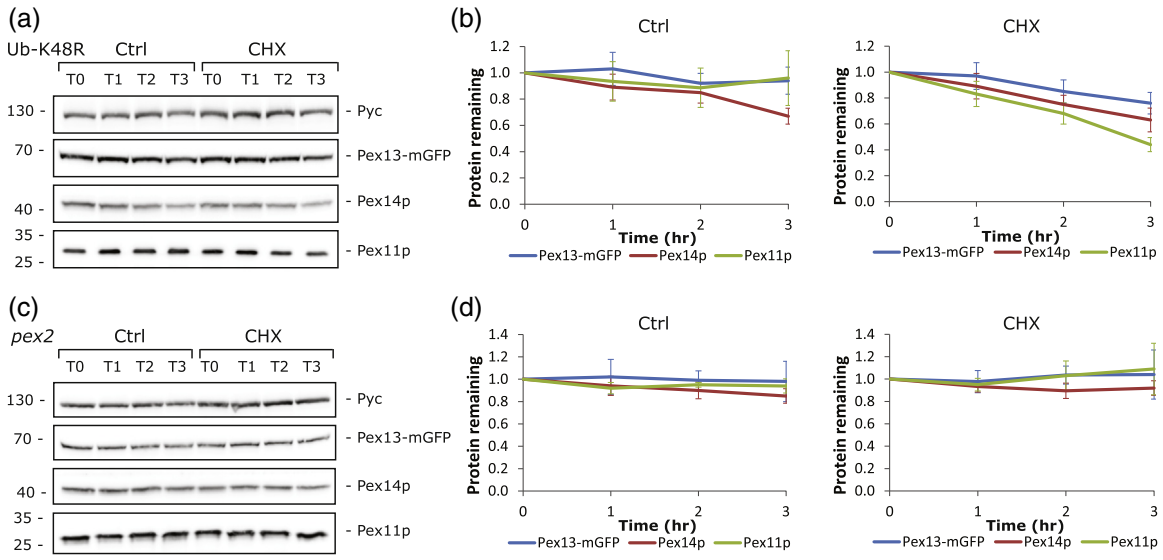

Fig. 3. Pex13p degradation is inhibited in *pex2Δ* or Ub-K48R cells. (a) Ub-K48R cells expressing Pex13-mGFP were grown on methanol/glycerol media for 12 h and treated with DMSO (Ctrl) or CHX. TCA samples were taken at the indicated time (h) after DMSO/CHX addition and probed by SDS-PAGE and immunoblotting with antibodies against mGFP, Pex14p, Pex11p and Pyc. (b) Quantification of Pex13-mGFP, Pex14p and Pex11p levels in Ub-K48R cells expressing Pex13-mGFP. Protein levels were normalized to the loading control Pyc. Protein levels at T0 were set to 1. Values represent the mean ± SD of three independent experiments. (c) Representative Western blots of *pex2Δ* cells expressing Pex13-mGFP derived from cells grown and treated as in panel a. Samples were probed with SDS-PAGE and immunoblotting with antibodies against mGFP, Pex11p and Pyc. (d) Quantification of protein levels in *pex2Δ* cells expressing Pex13-mGFP. Protein levels were normalized to Pyc. Protein levels at T0 were set to 1. Values represent the mean ± SD of three independent experiments. The blots used to quantify protein levels for panels b and d can be found in Figure S3.

Pex13p is ubiquitinated in WT cells, while Pex13p ubiquitination is reduced in pex2Δ cells

To investigate more directly the role of Ub and the peroxisomal E3 ligase complex in Pex13p degradation, we assessed whether Pex13p is ubiquitinated. To achieve this, we introduced a C-terminal His_6 tagged form of Pex13p into WT and *pex2Δ* cells and performed pull-down assays (Fig. 4). Cells also co-produced an Myc-tagged form of Ub (Myc-Ub), to aid detection of ubiquitinated proteins. A ladder of Myc-Ub Pex13-His_6 was detected in elution fractions isolated from WT cells co-expressing Pex13-His_6 and Myc-Ub (Fig. 4b, lane 4). This ladder was severely reduced in elution fractions isolated from *pex2Δ* cells co-expressing Pex13-His_6 and Myc-Ub (Fig. 4b, lane 3), providing direct evidence that Pex13p is ubiquitinated in WT cells and also showing that Pex13p ubiquitination requires the peroxisomal E3 ligase complex.

Pex5p, Pex14p and Pex8p play a role in Pex13p degradation

Next we sought to identify whether additional proteins are required for Pex13p degradation and focussed on proteins that were shown to interact with Pex13p in other organisms. These included the PTS1 receptor protein Pex5p [36], the docking factor Pex14p [37], the PTS2 receptor Pex7p [38] and its accompanying co-receptor protein Pex20p [38] and the cargo-dissociation factor Pex8p [39]. Deletion of genes that encode for proteins specifically involved in PTS2 protein import did not impact on Pex13p degradation (Fig. 5a and c) whereas Pex13p levels were increased around 3-fold in cells deleted for PEX5 and around 6-fold in cells deleted for PEX14 (Fig. 5a–c). Strikingly, PEX8 deletion resulted in a strong inhibition of Pex13p degradation, at a level comparable with that observed for *pex2Δ* cells (Fig. 5b and c). Pex14p levels were also increased in cells deleted for PEX8, although to a much lower extent, similar to in cells deleted for PEX2 (Figs. 1b and 5c). Deletion of PEX5, PEX8 or PEX14 did not affect PEX13 promotor activity (Fig. 1d), indicating that the increased levels of Pex13p indeed stem from inhibited protein degradation. We also observed what appeared to be modified forms of Pex13p in samples derived from *pex5Δ*, *pex14Δ*, *pex2Δ* or *pex8Δ* cells (denoted with a # in Fig. 5a and b). We consider it highly unlikely that these represent ubiquitinated forms of Pex13p, because deletion of PEX2 inhibits Pex13p ubiquitination (Fig. 4), which leaves us to conclude that they represent another modified form of Pex13p that becomes visible because Pex13p levels are increased in these deletion strains. We can only speculate as to which modification this could

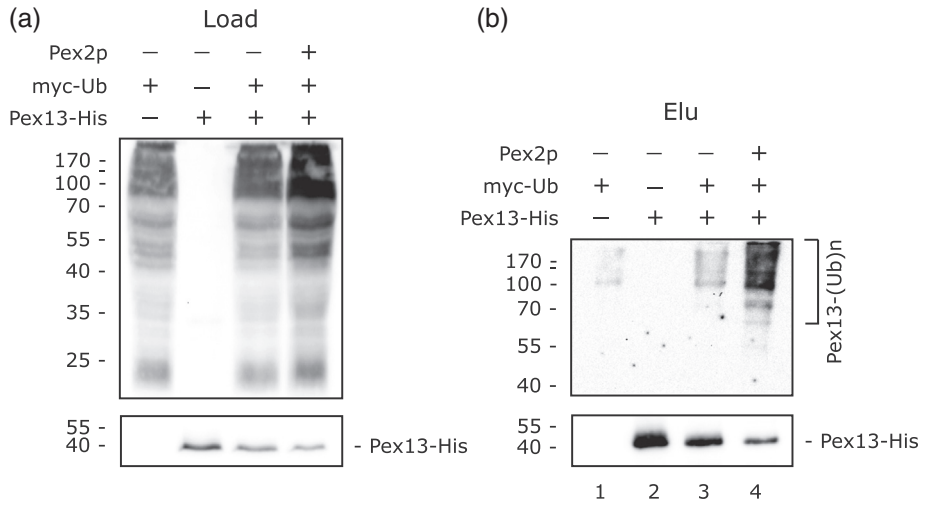

Fig. 4. Pex13p is ubiquitinated in WT cells, while Pex13p ubiquitination is reduced in *pex2Δ* cells. *pex2*/Myc-Ub, *pex2*/Pex13-His, *pex2*/Pex13-His/Myc-Ub and Pex13-His/Myc-Ub cells were grown on methanol/glycerol media for 12 h, and Pex13-His was purified under denaturing conditions using Ni-NTA resin. Load (a) and elution (b) fractions were subjected to SDS-PAGE and immunoblotting with antibodies raised against the Myc-tag (upper panels) or the His tag (lower panels).

represent but since phosphorylated Pex13p peptides have been found in mammalian cells [40], it may represent phosphorylated Pex13p.

Taken together, these observations demonstrate that additional factors are likely to play a role in Pex13p degradation.

Pex13-mGFP builds up at the peroxisomal membrane in pex2Δ cells

Our data could suggest that Pex13p is ubiquitinated by the peroxisomal ubiquitination machinery for proteasomal-mediated degradation. Since this machinery is present at the peroxisomal membrane and proteasomes are mostly cytosolic [41], we considered it likely that Pex13p would build up at the peroxisomal membrane when its degradation is inhibited. To investigate this further, we compared the behavior of Pex13-mGFP in WT and *pex2Δ* cells using fluorescence microscopy. Cells also co-produced Pex14-mKate2, to mark peroxisomes. Both Pex13-mGFP and Pex14-mKate2 co-localized in WT cells (Fig. 6a and b). *pex2Δ* cells lack functional peroxisomes, because Pex2p is required for matrix protein import [42]. Instead, *pex2Δ* cells contain peroxisome "ghosts," which are small peroxisomal membrane structures that contain most PMPs but very few matrix proteins [42]. Pex13-mGFP co-localized with Pex14-mKate2 in peroxisomal ghosts in *pex2Δ* cells (Fig. 6a and b), indicating that Pex13-mGFP associates with peroxisomes in *pex2Δ* cells. Furthermore, *pex2Δ* cells displayed an increase in GFP intensity (Fig. 6c) as well as an increased mGFP/mKate2 intensity ratio (Fig. 6d), compared to WT cells, confirming that Pex13-mGFP protein levels are elevated in *pex2Δ* cells (Fig. 6e). Note that in Fig. 6a, fluorence images were processed with optimal settings to clearly show signals, while images in Fig. 6b were processed to reflect the difference in fluorescence intensities between the two strains. Taken together, these results indeed confirm that Pex13-mGFP builds up at the peroxisomal membrane in the absence of a functional peroxisomal E3 ligase complex.

Discussion

The molecular function of the peroxisomal ubiquitination machinery was long thought to be restricted to cycling receptor ubiquitination. However, several recent reports have identified additional roles for this machinery in peroxisome biology. Here, we present data that suggest a role for the E2 Pex4p and the RING E3 ligases Pex2p, Pex10p and Pex12p in the degradation of Pex13p, while we also provide evidence that Pex13p is ubiquitinated in a manner that requires a functional peroxisomal E3 ligase complex. Following this line of reasoning, our data suggest a model where Pex13p is ubiquitinated by Pex4p and the peroxisomal E3 ligase complex to target Pex13p for proteasomal-mediated degradation. While this model is an attractive proposal, it remains hypothetical at the current time because we have not shown that the peroxisomal ubiquitination machinery is directly involved in Pex13p ubiquitination. Such evidence will likely come from the use of assays that reconstitute the ubiquitination of Pex13p *in vitro*. Nevertheless our data, when coupled together with the observations that Pex5p [13,14], members of the

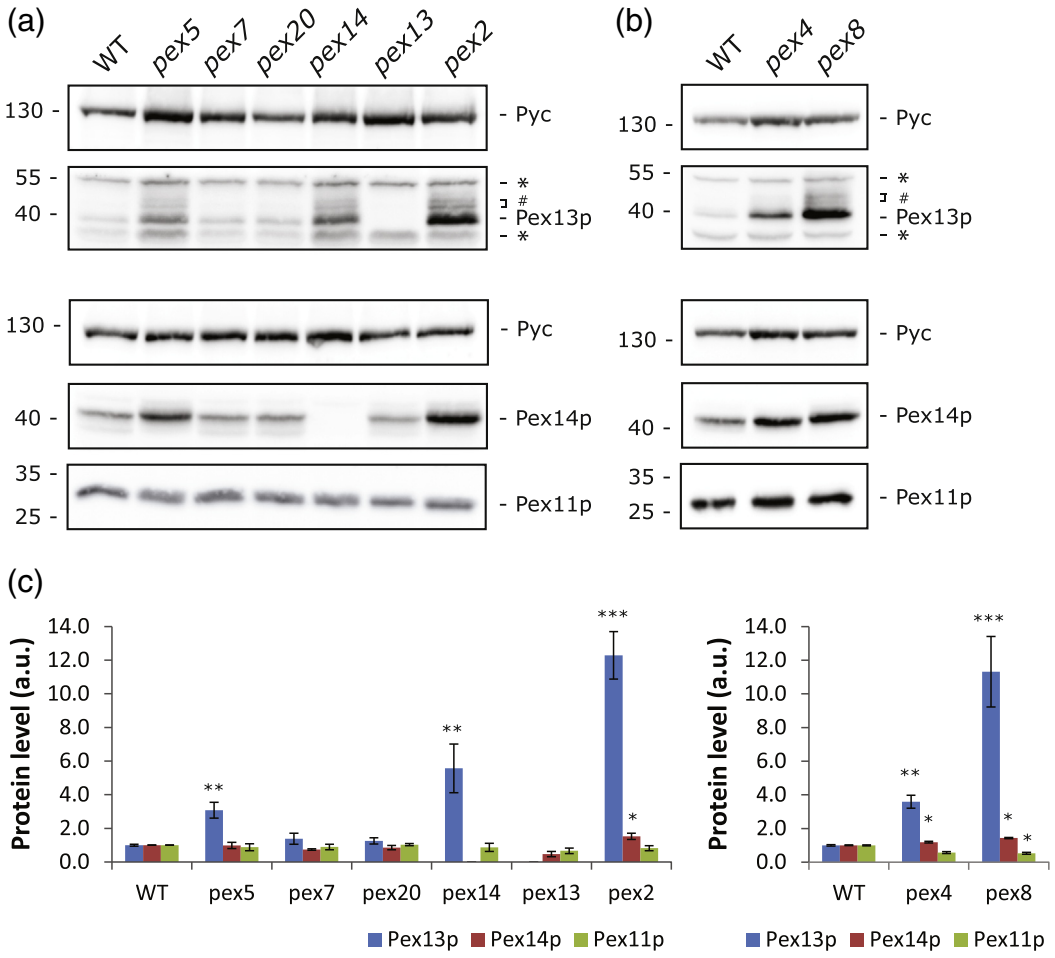

Fig. 5. Pex13p levels are elevated in *pex5Δ*, *pex14Δ* and *pex8Δ* cells. (a) Representative Western blots of samples derived from WT and mutant cells grown for 16 h on methanol/glycerol media. Blots were probed with antibodies directed against Pex13p, Pex14p, Pex11p and Pyc. * Denotes anti-Pex13p cross reactive species. (b) Lysates from WT, *pex4Δ* and *pex8Δ* cells (grown as in panel a) were subjected to SDS-PAGE and immunoblotting using antibodies against Pex13p, Pex14p, Pex11p and Pyc. * Denotes anti-Pex13p cross-reactive species. (c) Quantification of protein levels in WT and mutant cells, normalized to the loading control Pyc. Protein levels in WT cells were set to 1. Values represent the mean ± SD of three independent experiments. Asterisks denote statistically significant increases in protein levels compared to those in WT samples (*$P < 0.05$, **$P < 0.01$, ***$P < 0.001$). The blots used to quantify protein levels for panel c can be found in Figure S4.

Pex20p family [22,43] and Pex7p [44] can all be ubiquitinated for proteasomal-mediated degradation, indicate that the UPS is involved in targeting a range of peroxisomal proteins for degradation, suggesting a determining role for the UPS in regulating peroxisome function.

This leads to the question: Why is Pex13p targeted for degradation? Currently, it is only possible to speculate on this. Since Pex13p is essential for peroxisomal matrix protein import [25], degradation of Pex13p would likely inhibit the import process. In this light, an interesting comparison can be drawn with recent work on *Arabidopsis* Pex13p [45]. Here, the authors reported that *Arabidopsis* Pex13p can be degraded by the RING E3 Ligase SP1 *in vivo*. SP1 also facilitates the ubiquitination and degradation of TOC (translocon at the outer envelope of chloroplasts) complexes, controlling the import of proteins into chloroplasts [46]. While a role for SP1 in peroxisomes remains controversial [47,48], our data would fit a model similar to the one proposed by Pan *et al.* [45], which suggests that Pex13p degradation negatively regulates peroxisomal matrix protein import by down-regulating import complexes on the peroxisomal membrane. Alternatively, the peroxisomal ubiquitination machinery may target damaged or incorrectly folded Pex13p for degradation, in a similar way to the endoplasmic reticulum-associated degradation (ERAD) pathway [49]. Either way, we predict that Pex13p degradation will impact on peroxisomal matrix

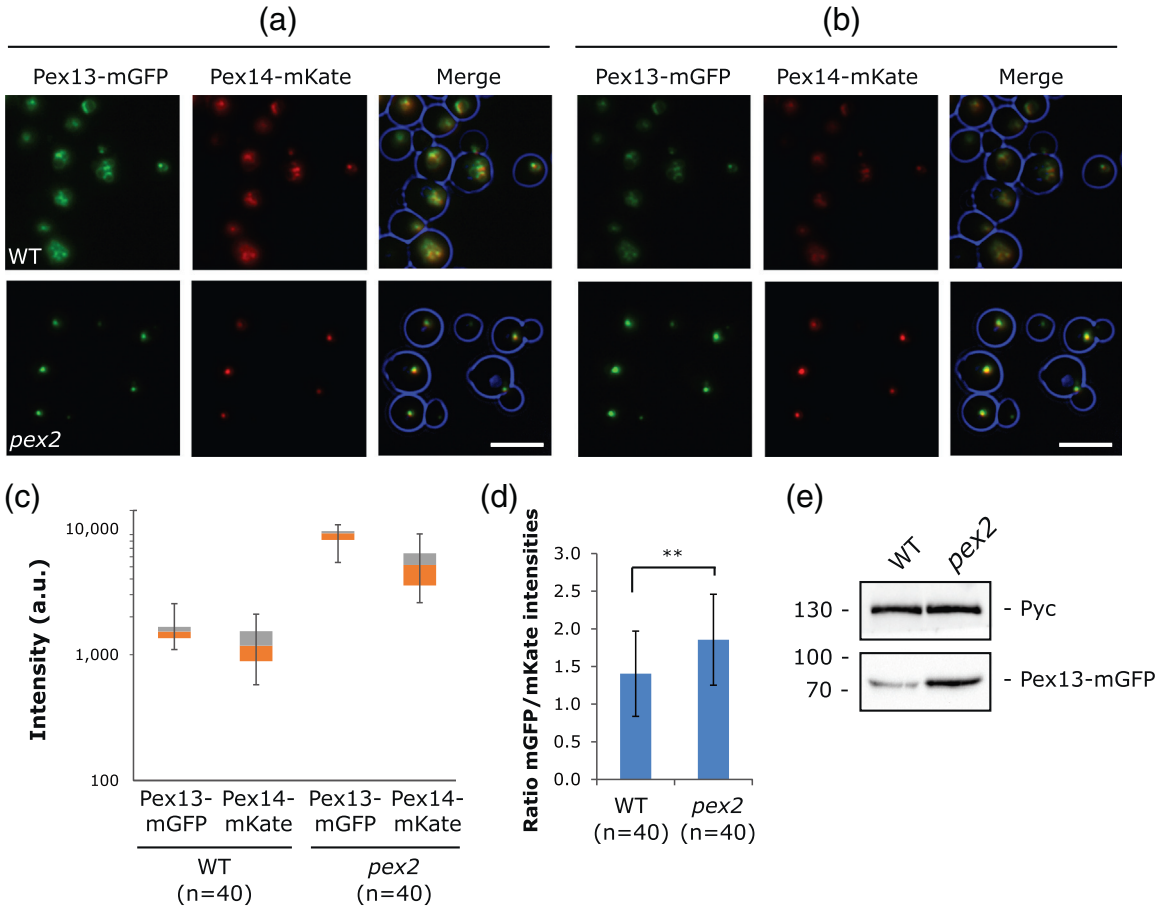

Fig. 6. Pex13-mGFP accumulates on the peroxisomal membrane in *pex2Δ* cells. (a) WT and *pex2Δ* cells producing Pex13-mGFP and Pex14-mKate2 were grown on methanol/glycerol media to an OD_{600} of 1.0 and fluorescence microscopy images were taken. Images of Pex13-mGFP were processed using ImageJ with optimal settings to show signals in WT and *pex2Δ*. Pex14-mKate2 was used as a peroxisomal membrane marker. The following settings were used: for WT cells, mGFP (255, 2500) and mKate2 (219, 3000); for *pex2* cells, mGFP (255, 7000) and mKate2 (219, 4700). The scale bar represents 5 μm. (b) Fluorescence images of Pex13-mGFP in WT or *pex2Δ* shown in panel a were processed using ImageJ with the same settings: mGFP (255, 5000), mKate2 (219, 4000). The scale bar represents 5 μm. (c) Box plot showing quantification of mGFP and mKate2 fluorescence intensity at the peroxisomal membrane in WT and *pex2Δ* cells producing Pex13-mGFP and Pex14-mKate2. Fluorescence intensities (auxiliary units) were measured using ImageJ. The box represents values from the 25 percentile to the 75 percentile; the horizontal line through the box represents the median value. Whiskers indicate maximum and minimum values. mGFP and mKate2 measurements were taken as described in the Materials and Methods section. (d) Average ratio ± SD per cell (n = 40) of mGFP to mKate intensities in WT and *pex2Δ* cells. $^{**}P < 0.01$. (E) WT and *pex2Δ* cells producing Pex13-mGFP were grown on methanol/glycerol media and TCA samples were taken when the cultures reached an OD_{600} of 1.0. Samples were subjected to SDS-PAGE and immunoblotting using antibodies against mGFP and Pyc.

protein import, making it an interesting topic for further study.

Our data also indicate a role for the cycling receptor Pex5p, the docking protein Pex14p and the intraperoxisomal protein Pex8p in Pex13p degradation. How these proteins may be involved in Pex13p degradation is unclear at the current time, although the involvement of Pex5p and Pex14p could suggest that Pex13p degradation is linked to PTS1 protein import. Likewise, the effect of deleting PEX8 on Pex13p degradation could also suggest a link to PTS1 protein import. However, this may stem from a different reason. Pex13p binds to Pex8p and this interaction was proposed to allow the docking complex, consisting of Pex13p, Pex14p and Pex17p, to contact the E3 ligase complex consisting of Pex2p, Pex10p and Pex12p [29]. Such a model would suggest that Pex13p and the E3 ligase complex are unable to associate in cells deleted for PEX8, which may result in a block to Pex13p ubiquitination and hence degradation. The increase in Pex13p levels in *pex8Δ* and *pex2Δ* cells is comparable (Fig. 5), which may suggest that deleting

PEX2 or PEX8 impacts on the same aspect of Pex13p degradation, although further data will be required to validate this theory.

Deletion of PEX4 does not impact on Pex13p levels to the same extent as deletion of a member of the peroxisomal E3 ligase complex (Fig. 1). Pex13p degradation appears completely blocked in *pex2Δ* cells (Fig. 3), which leads us to conclude that Pex13p degradation is not fully inhibited in cells lacking Pex4p. This could suggest that another E2 enzyme, together with the peroxisomal E3 ligase complex, promotes Pex13p ubiquitination and degradation in *pex4Δ* cells, albeit at an apparently lower level. While we can only speculate as to the identity of the E2 in this model, the fact that Ubc4p has been implicated in the ubiquitination and degradation of peroxisomal proteins and can serve as E2 with the peroxisomal E3 ligase complex [16,50,51] makes it a possible candidate.

In summary, our results add strong support to the idea that the peroxisomal ubiquitination machinery is not only required for ubiquitinating Pex5p and members of the Pex20p family, but it also targets additional peroxisomal proteins. Indeed, members of the peroxisomal E3 ligase complex are now linked to the ubiquitination/degradation of Pex13p (this study), pexophagy-induced Pex3p ubiquitination/degradation in *H. polymorpha* [19] and the ubiquitination of PMP70 in mammals [21]. In addition, Pex4p is required for the degradation of the peroxisomal matrix proteins ICL and MLS in plants [52], Pex18p degradation in *S. cerevisiae* [22] and Pex20p degradation in *Pichia pastoris* [43] while when in complex with its membrane anchor Pex22p, Pex4p from both *S. cerevisiae* and *H. polymorpha* is able to produce K48 linked Ub chains *in vitro* [53,54], which suggests a role for Pex4p in proteasomal-mediated degradation. However, as with Pex13p, further evidence that these proteins are *bona fide* substrates of the peroxisomal ubiquitination machinery is still required. Nevertheless, the results presented here, together with the above-mentioned reports, lead us to propose that the peroxisomal ubiquitination machinery, rather than simply being involved in receptor recycling, in fact functions as a platform that facilitates the ubiquitination of an array of peroxisomal proteins, regulating peroxisome biology through the ubiquitination/degradation of peroxisomal proteins. Therefore, we anticipate that many more substrates of this machinery remain to be discovered.

Materials and Methods

Molecular techniques and construction of *H. polymorpha* strains

Transformation of *H. polymorpha* was performed by electroporation as described previously [55]. *H. polymorpha* strains used in list study are listed in Table S1. The plasmids and primers used in this study are listed in Table S2 and S3, respectively. Phusion DNA polymerase (Thermo Scientific) was used to produce gene fragments.

The *Escherichia coli* vector for expression of the SH3 domain of Pex13p, complete with N-terminal His_6-tag (pCW360) was made as follows: PCR was performed on *H. polymorpha* genomic DNA using the primer combinations P13 SH3 F and P13 SH3 R, and the resulting fragment was digested with NcoI and HindIII and ligated *into NcoI-HindIII* digested pETM11.

The *H. polymorpha aox* strain was made by Gateway cloning (Invitrogen). The 5′fragment of the *AOX* promoter (P_{AOX}) was amplified with from genomic DNA using primers attAOXp-5′ UP and attAOXp-5′ DN. The 3′fragment of AOXp, complete with start of the coding region on the AOX gene, was amplified from *H. polymorpha* genomic DNA with primers att-AOX-3′ UP and att-AOX-3′ DN. Each PCR product was used for the BP reaction to ligate into pENTR to generate pENTR-AOXp and pENTR-3′ AOXp. Plasmids pENTR-AOXp, pENTR-URA, pENTR-3′AOXp and pDEST-R4R3 were used for LR reaction to generate pDEST-deltaAOX(URA). The product was digested with PstI and BglII to generate two fragments of 2.3 and 2.5 kb. The 2.3-kb fragment was used for *H. polymorpha* transformation.

To construct pHIPZ20-mGFP, the PEX13 promoter (P_{PEX13}) was amplified from WT genomic DNA with primers Pro-P13-NotI-F and Pro-P13-SalI-R, and cloned into pHIPZ6-Pex3-His_6 [19] replacing the P_{PEX3}-Pex3-His_6 fragment between NotI and SalI sites to generate pHIPZ20. mGFP was amplified from Pex13-mGFP with primers SalI-GFP-F and GFP-XbaI-R and cloned into pHIPZ20 between SalI and XbaI sites. To construct pHIPZ20-Pex13-His_6, a Pex13 fragment of was amplified from WT genomic DNA with primers SalI-P13-F and P13-His6-XbaI-R, which incorporated a sequence encoding for a C-terminal His_6 tag into the DNA fragment, and cloned into pHIPZ20-mGFP, replacing mGFP between the SalI and XbaI sites. All plasmids containing P_{PEX13} were linearized with NheI prior to transformation into *H. polymorpha* cells.

The plasmid pHIPH-Pex14-mKate2 was constructed as follows: PCR was performed on the plasmid pFA6 yomKate2-CaURA3 (Addgene plasmid no. 44878) using primers yomKate2 fw and yomKate2 rev, and the resulting mKate2 DNA fragment was digested with BglII and SphI and ligated into BglII-SphI digested pSNA12 [56], producing pHIPZ-Pex14-mKate2. This vector was linearized with PstI and transformed into *H. polymorpha* WT cells. Next, genomic DNA was isolated from WT Pex14-mKate2 (Zeo) cells and used as template for a PCR reaction using primers Pex14-F and Pex14-SpeI-R, and the DNA fragment was digested with BamHI and XmaI and ligated into BamHI-XmaI digested pSEM04 [35], producing pHIPH5-Pex14-mKate2. This vector was

then digested with NotI and BamHI to remove AMO promoter fragment and the product was treated with Klenow fragment to produce blunt-ends. Following this, the blunt ends were ligated together, forming the plasmid pHIPH-Pex14-mKate2. pHIPH-Pex14-mKate2 was linearized with Bpu1102I prior to transformation into *H. polymorpha* cells.

The pHIPZ-Pex13-mGFP plasmid [35] was linearized with ApaI prior to transformation into *H. polymorpha* cells.

All integrations were confirmed by colony PCR using Phire Hot Start II (Thermo Scientific), and *pex2* pHIPZ20-mGFP, *pex4* pHIPZ20-mGFP, *pex5* pHIPZ20-mGFP, *pex8* pHIPZ20-mGFP, *pex14* pHIPZ20-mGFP, Myc-Ub-K48R pHIPZ20-mGFP, WT pHIPZ20-mGFP and PEX13-His_6 were further checked with Southern blotting.

Southern blotting

Southern blotting analysis was performed using the DIG Direct Nucleic Acid Labelling and Detection system (Roche) according to the established methods. *H. polymorpha* genomic DNA containing the integrated plasmid PHIPZ20-mGFP was digested with NdeI (Thermo Scientific), while *H. polymorpha* genomic DNA containing the integrated pHIPZ20-Pex13-His_6 plasmid was digested with EcoRI (Thermo Scientific). The probe for P_{PEX13}-mGFP, consisting of a 0.5-kb fragment upstream to PEX13, was amplified using Pp13GFP-S-ProbeF and Pp13GFP-S-ProbeR. The probe for Pex13-His_6, consisting of a 0.5-kb fragment 1 kb upstream, was amplified using primers Sthn-13(R)CSProbF and Sthn-13(R)CSProbR. The probe recognizes a 2.5-kb fragment in *pex13Δ* cells and an ~8-kb fragment in one-copy mutant cells.

Strains and growth conditions

Yeast transformants were selected on YPD plates containing 2% agar and 100 μg/ml Zeocin (Invitrogen) or 300 μg/ml Hygromycin (Invitrogen) or on YND plates containing 2% agar, for production of the *aox* deletion strain. The *E. coli* strain DH5α was used for cloning purposes. *E. coli* cells were grown in LB supplemented with 100 μg/ml Ampicillin at 37 °C. *H. polymorpha* cells were grown in batch cultures at 37 °C on mineral media supplemented with 0.25% glucose or 0.5% methanol with 0.05% glycerol as carbon source and 0.25% ammonium sulfate or 0.25% methylamine as nitrogen source. Leucine, when required, was added to a final concentration of 30 μg/ml. CHX, when used, was added to a final concentration of 6 mg/ml.

Preparation of yeasts TCA lysates for Western blotting

Cell extracts of TCA-treated cells were prepared for SDS-PAGE as detailed previously [57]. Equal amounts of protein were loaded per lane and blots were probed with rabbit polyclonal antisera raised against the Myc tag (Santa Cruz Biotech, sc-789), Pex13p (Figure S5), Pex14p [58], Pex11p [35] or pyruvate carboxylase 1 (Pyc) [59] or mouse monoclonal antisera raised against penta-His tag (Qiagen, 34660) or mGFP (Santa Cruz Biotech, sc-9996). Secondary goat anti-rabbit (31460) or goat anti-mouse (31430) antibodies conjugated to horseradish peroxidase (Thermo Scientific) were used for detection. Pyc was used as a loading control. Note that the anti-Pex14p can recognize both the phosphorylated (upper band) and unphosphorylated (lower band) forms of Pex14p.

Expression and purification of Pex13p SH3 for antibody production

The SH3 domain of *H. polymorpha* Pex13p with a cleavable His_6-tag was produced in the *E. coli* strain BL21 (DE3) RIL. Cells were grown at 37 °C to an OD600 of 1.0 in Terrific Broth medium supplemented with antibiotics, transferred to 20 °C and grown until an OD600 of 1.5. Protein expression was then induced with 0.04mM IPTG (Invitrogen) for 16 h and cells were harvested by centrifugation. *E. coli* cell pellets expressing His_6-Pex13 SH3 were thawed in lysis buffer [50 mM Tris–HCl (pH 7.5), 300 mM NaCl, 10 mM imidazole, 2 mM β-mercaptoethanol] and passed through a French press. Cell debris was removed by centrifugation and lysates were loaded onto glutathione Ni-NTA resin (Fisher Scientific) pre-equilibrated with lysis buffer. The resin was extensively washed with lysis buffer, wash buffer 1 (50mM Tris, 1 M NaCl, 20 mM imidazole and 1 mM β-mercaptoethanol) and wash buffer 2 (50 mM Tris, 300 mM NaCl, 40 mM imidazole and 1 mM β-mercaptoethanol), and His_6-Pex13 SH3 was eluted with elution buffer (50 mM Tris, 150 mM NaCl, 330 mM imidazole and 1 mM β-mercaptoethanol). Finally, purified His_6-Pex13 SH3 was passed over a PD10 column (GE Healthcare) equilibrated in PD10 buffer (50 mM Tris, 150 mM NaCl and 1 mM β-mercaptoethanol) to remove the imidazole. After confirming presence of the purified protein using SDS-PAGE, protein samples were sent for antibody production (Eurogentec). The properties of the resulting anti-Pex13p antibodies are shown in Figure S5.

Quantification of Western blots

Blots were scanned by using a densitometer (GS-710; Bio-Rad Laboratories) and protein levels were quantified using Image Studio Lite Ver5.2 software (LI-COR Biosciences). In the case of Pex14p blots, both the phosphorylated and unphosphorylated forms were included in the calculation if both forms were visible. The value obtained for each band was normalized by dividing it by the value of the corresponding Pyc band (loading control). For

comparison of absolute protein levels (Figs. 1 and 5), normalized values obtained for Pex13p, Pex14p and Pex11p levels in WT cells were set to 1 and the levels of these proteins in mutant cells are displayed relative to WT. For CHX experiments (Figs. 2 and 3), the normalized values of T0 samples were set to 1.0 and values obtained from the T1–T3 samples are displayed as a fraction of T0 values. Standard deviations were calculated using Excel. Significance was determined using IBM SPSS Statistics 23 software (IBM), employing the function analyze-compare means-independent samples *t*-test (with Levene test for deviation homogeneity). * represents P values < 0.05, ** represents P values < 0.01 and *** represents P values < 0.001. The data presented are derived from three independent experiments.

Pull-down assay

Cells were grown at 37 °C to the mid-exponential growth phase (~8 h) in 200 ml mineral medium containing 0.5% methanol and 0.05% glycerol, and 50 OD_{600} units of cells of each strain were harvested by centrifugation. Cells were washed once with demineralized water and resuspended in Equilibrium buffer [50 mM potassium phosphate buffer (pH 7.2), 10 mM imidazole, 10 mM iodoacetamide, 5 mM *N*-ethylmaleimide, 1 mM PMSF added just prior to use, and 2.5 μg/ml leupeptin]. The preparation of crude extracts of yeast cells using glass beads was performed as previously described [60]. Samples of cell homogenates were then treated for 30 min at room temperature with final concentration of 8 M urea and 1.0% Triton X-100 (Sigma) to denature proteins and solubilize membranes. Samples were briefly centrifuged at 4000*g* to remove unbroken cells and lysates were incubated with Ni-NTA resin (QIAGEN) for 60 min at room temperature, with gentle shaking. The resin was then sequentially washed with Wash buffer 1 [50 mM potassium phosphate buffer (pH 7.2), 40 mM imidazole, 6 M urea, 10 mM iodoacetamide, 5 mM *N*-ethylmaleimide, 1 mM PMSF added just prior to use, and 2.5 μg/ml leupeptin] and Wash buffer 2 [50 mM potassium phosphate buffer (pH 7.2), 40 mM imidazole, 6 M urea, 1.0% Triton X-100, 10 mM iodoacetamide, 5 mM *N*-ethylmaleimide, 1 mM PMSF added just prior to use, and 2.5 μg/ml leupeptin]. The resin was then transferred to new tube, all liquid was removed with syringe and proteins were eluted with SDS-PAGE loading buffer (without β-mercaptoethanol) at 37 °C for 10 min.

Fluorescence microscopy

All fluorescence microscopy images were acquired using a 100 × 1.30 NA Plan-Neofluar objective (Carl Zeiss). Wide-field microscopy images were captured by an inverted microscope (Axio Scope A1, Carl Zeiss) using Micro-Manager software and a digital camera (CoolSNAP HQ [2]; Photometrics). GFP signal was visualized with a 470/440-nm band-pass excitation filter, a 495-nm dichromatic mirror and 525/550-nm band-pass emission filter.

For images taken of Pex13-mGFP in WT grown on methanol/glycerol mineral medium, the optimal settings were mGFP (255, 2500) and mKate2 (219, 3000), and in *pex2*, the optimal settings mGFP (255, 7000) and mKate2 (219, 4700) were applied for processing. The general settings used to compare the signal of Pex13-mGFP in WT and *pex2*, mGFP (255, 5000) and mKate2 (219, 4000) were applied for processing.

For quantification of the Pex13-mGFP or Pex14-mKate2 intensities in individual WT or *pex2* cells ($n = 40$), a rectangular area was drawn using the "rectangular tool" from ImageJ [61] to envelope the region containing the Pex13-mGFP/Pex14-mKate2 spot and pixel intensity inside the area was measured. The measured maximum fluorescence intensity of GFP or mKate2 on peroxisomes was corrected for the background intensity and a box plot was made using Microsoft Excel. The box represents values from the 25 percentile to the 75 percentile; the horizontal line through the box represents the median value. Whiskers indicate maximum and minimum values. To obtain the average ratio of mGFP/mKate intensities per cell (Fig. 6d), the maximum mGFP intensity was divided by the maximum mKate2 intensity for each cell and the average ± SD over all cells was plotted. Microsoft Excel was used to determine significance. ** represents P values < 0.01.

Acknowledgments

The authors thank Joana Neto-Gomes, Ida van der Klei, Thomas Schroeter, Jessica Kluemper, Wolfgang Schliebs and Ralf Erdmann for helpful discussions; Arjen Krikken for advice with processing of fluorescence microscopy images; and Jan Kiel for critically reading the manuscript. This work was funded by a VIDI Fellowship (723.013.004) from the Netherlands Organisation for Scientific Research (NWO), awarded to C.W.

Author Contributions: C.W. conceived and supervised the project. C.W., S.D., N.D. and X.C. designed the experiments. X.C., S.D., N.D. and C.W. analyzed the data. X.C. performed biochemical and fluorescence microscopy experiments, with support from S.D. and N.D. All authors discussed the results. X.C. and C.W. wrote the manuscript, with contributions from all authors.

Conflict of Interest: The authors declare no conflict of interest.

Appendix A. Supplementary data

Supplementary data to this article can be found online at https://doi.org/10.1016/j.jmb.2018.03.033.

Received 6 February 2018;
Received in revised form 15 March 2018;
Accepted 16 March 2018
Available online 22 April 2018

Keywords:
peroxisome;
protein degradation;
ubiquitin proteasome system;
PMP;
peroxisomal membrane protein

Current address: N. Danda, Institut du Cerveau et de la Moelle épinière (ICM), Hôpital Pitié-Salpêtrière, 47 bd de l'Hôpital, 75013 Paris, France.

Abbreviations used:
PMP, peroxisomal membrane protein; PTS, peroxisomal targeting signals; Ub, protein ubiquitin; WT, wild-type; UPS, ubiquitin–proteasome system; AOX, alcohol oxidase; CHX, cycloheximide.

References

[1] T. Gabaldon, Peroxisome diversity and evolution, Philos. Trans. R. Soc. Lond. Ser. B Biol. Sci. 365 (2010) 765–773.
[2] H.R. Waterham, S. Ferdinandusse, R.J. Wanders, Human disorders of peroxisome metabolism and biogenesis, Biochim. Biophys. Acta 1863 (2016) 922–933.
[3] P.U. Mayerhofer, Targeting and insertion of peroxisomal membrane proteins: ER trafficking versus direct delivery to peroxisomes, Biochim. Biophys. Acta 1863 (2016) 870–880.
[4] E.H. Hettema, S.J. Gould, Cell biology: organelle formation from scratch, Nature 542 (2017) 174–175.
[5] A. Baker, T.L. Hogg, S.L. Warriner, Peroxisome protein import: a complex journey, Biochem. Soc. Trans. 44 (2016) 783–789.
[6] C. Williams, W.A. Stanley, Peroxin 5: a cycling receptor for protein translocation into peroxisomes, Int. J. Biochem. Cell Biol. 42 (2010) 1771–1774.
[7] P.B. Lazarow, The import receptor Pex7p and the PTS2 targeting sequence, Biochim. Biophys. Acta 1763 (2006) 1599–1604.
[8] W. Schliebs, W.H. Kunau, PTS2 co-receptors: diverse proteins with common features, Biochim. Biophys. Acta 1763 (2006) 1605–1612.
[9] D. Komander, M. Rape, The ubiquitin code, Annu. Rev. Biochem. 81 (2012) 203–229.
[10] H.W. Platta, F. El Magraoui, D. Schlee, S. Grunau, W. Girzalsky, R. Erdmann, Ubiquitination of the peroxisomal import receptor Pex5p is required for its recycling, J. Cell Biol. 177 (2007) 197–204.
[11] C. Williams, M. van den Berg, R.R. Sprenger, B. Distel, A conserved cysteine is essential for Pex4p-dependent ubiquitination of the peroxisomal import receptor Pex5p, J. Biol. Chem. 282 (2007) 22534–22543.
[12] C.P. Grou, A.F. Carvalho, M.P. Pinto, S.J. Huybrechts, C. Sa-Miranda, M. Fransen, J.E. Azevedo, Properties of the ubiquitin–pex5p thiol ester conjugate, J. Biol. Chem. 284 (2009) 10504–10513.
[13] J.A. Kiel, K. Emmrich, H.E. Meyer, W.H. Kunau, Ubiquitination of the peroxisomal targeting signal type 1 receptor, Pex5p, suggests the presence of a quality control mechanism during peroxisomal matrix protein import, J. Biol. Chem. 280 (2005) 1921–1930.
[14] H.W. Platta, W. Girzalsky, R. Erdmann, Ubiquitination of the peroxisomal import receptor Pex5p, Biochem. J. 384 (2004) 37–45.
[15] F. El Magraoui, A. Schrotter, R. Brinkmeier, L. Kunst, T. Mastalski, T. Muller, K. Marcus, H.E. Meyer, W. Girzalsky, R. Erdmann, H.W. Platta, The cytosolic domain of Pex22p stimulates the Pex4p-dependent ubiquitination of the PTS1-receptor, PLoS One 9 (2014), e105894.
[16] C. Williams, M. van den Berg, E. Geers, B. Distel, Pex10p functions as an E3 ligase for the Ubc4p-dependent ubiquitination of Pex5p, Biochem. Biophys. Res. Commun. 374 (2008) 620–624.
[17] H.W. Platta, M.O. Debelyy, F. El Magraoui, R. Erdmann, The AAA peroxins Pex1p and Pex6p function as dislocases for the ubiquitinated peroxisomal import receptor Pex5p, Biochem. Soc. Trans. 36 (2008) 99–104.
[18] S. Leon, L. Zhang, W.H. McDonald, J. Yates III, J.M. Cregg, S. Subramani, Dynamics of the peroxisomal import cycle of PpPex20p: ubiquitin-dependent localization and regulation, J. Cell Biol. 172 (2006) 67–78.
[19] C. Williams, I.J. van der Klei, Pexophagy-linked degradation of the peroxisomal membrane protein Pex3p involves the ubiquitin–proteasome system, Biochem. Biophys. Res. Commun. 438 (2013) 395–401.
[20] A.R. Bellu, F.A. Salomons, J.A. Kiel, M. Veenhuis, I.J. Van Der Klei, Removal of Pex3p is an important initial stage in selective peroxisome degradation in *Hansenula polymorpha*, J. Biol. Chem. 277 (2002) 42875–42880.
[21] G. Sargent, T. van Zutphen, T. Shatseva, L. Zhang, V. Di Giovanni, R. Bandsma, P.K. Kim, PEX2 is the E3 ubiquitin ligase required for pexophagy during starvation, J. Cell Biol. 214 (2016) 677–690.
[22] P.E. Purdue, P.B. Lazarow, Pex18p is constitutively degraded during peroxisome biogenesis, J. Biol. Chem. 276 (2001) 47684–47689.
[23] C. Williams, Going against the flow: a case for peroxisomal protein export, Biochim. Biophys. Acta, Mol. Cell Res. 1843 (2014) 1386–1392.
[24] J.E. Azevedo, W. Schliebs, Pex14p, more than just a docking protein, Biochim. Biophys. Acta 1763 (2006) 1574–1584.
[25] C. Williams, B. Distel, Pex13p: docking or cargo handling protein? Biochim. Biophys. Acta 1763 (2006) 1585–1591.
[26] F.L. Theodoulou, K. Bernhardt, N. Linka, A. Baker, Peroxisome membrane proteins: multiple trafficking routes and multiple functions? Biochem. J. 451 (2013) 345–352.
[27] M. Schrader, J.L. Costello, L.F. Godinho, A.S. Azadi, M. Islinger, Proliferation and fission of peroxisomes—an update, Biochim. Biophys. Acta 1863 (2016) 971–983.
[28] J.S. Thrower, L. Hoffman, M. Rechsteiner, C.M. Pickart, Recognition of the polyubiquitin proteolytic signal, EMBO J. 19 (2000) 94–102.
[29] B. Agne, N.M. Meindl, K. Niederhoff, H. Einwachter, P. Rehling, A. Sickmann, H.E. Meyer, W. Girzalsky, W.H.

Kunau, Pex8p: an intraperoxisomal organizer of the peroxisomal import machinery, Mol. Cell 11 (2003) 635–646.
[30] J.M. Cregg, I.J. van der Klei, G.J. Sulter, M. Veenhuis, W. Harder, Peroxisome deficient mutants of *Hansenula polymorpha*, Yeast 6 (1990) 87–97.
[31] I.J. van der Klei, H. Yurimoto, Y. Sakai, M. Veenhuis, The significance of peroxisomes in methanol metabolism in methylotrophic yeast, Biochim. Biophys. Acta 1763 (2006) 1453–1462.
[32] G. Kleiger, T. Mayor, Perilous journey: a tour of the ubiquitin–proteasome system, Trends Cell Biol. 24 (2014) 352–359.
[33] P. Boya, F. Reggiori, P. Codogno, Emerging regulation and functions of autophagy, Nat. Cell Biol. 15 (2013) 713–720.
[34] C. Park, A.M. Cuervo, Selective autophagy: talking with the UPS, Cell Biochem. Biophys. 67 (2013) 3–13.
[35] K. Knoops, S. Manivannan, M.N. Cepinska, A. Krikken, A.M. Kram, M. Veenhuis, I.J. Van der Klei, Preperoxisomal vesicles can form in the absence of Pex3p, J. Cell Biol. 204 (2014) 659–668.
[36] A. Douangamath, F.V. Filipp, A.T. Klein, P. Barnett, P. Zou, T. Voorn-Brouwer, M.C. Vega, O.M. Mayans, M. Sattler, B. Distel, M. Wilmanns, Topography for independent binding of alpha-helical and PPII-helical ligands to a peroxisomal SH3 domain, Mol. Cell 10 (2002) 1007–1017.
[37] J.R. Pires, X. Hong, C. Brockmann, R. Volkmer-Engert, J. Schneider-Mergener, H. Oschkinat, R. Erdmann, The ScPex13p SH3 domain exposes two distinct binding sites for Pex5p and Pex14p, J. Mol. Biol. 326 (2003) 1427–1435.
[38] K. Stein, A. Schell-Steven, R. Erdmann, H. Rottensteiner, Interactions of Pex7p and Pex18p/Pex21p with the peroxisomal docking machinery: implications for the first steps in PTS2 protein import, Mol. Cell. Biol. 22 (2002) 6056–6069.
[39] M. Deckers, K. Emmrich, W. Girzalsky, W.L. Awa, W.H. Kunau, R. Erdmann, Targeting of Pex8p to the peroxisomal importomer, Eur. J. Cell Biol. 89 (2010) 924–931.
[40] K. Sharma, R.C. D'Souza, S. Tyanova, C. Schaab, J.R. Wisniewski, J. Cox, M. Mann, Ultradeep human phosphoproteome reveals a distinct regulatory nature of Tyr and Ser/Thr-based signaling, Cell Rep. 8 (2014) 1583–1594.
[41] C. Wojcik, G.N. DeMartino, Intracellular localization of proteasomes, Int. J. Biochem. Cell Biol. 35 (2003) 579–589.
[42] A. Koek, M. Komori, M. Veenhuis, I.J. van der Klei, A comparative study of peroxisomal structures in *Hansenula polymorpha* pex mutants, FEMS Yeast Res. 7 (2007) 1126–1133.
[43] X. Liu, S. Subramani, Unique requirements for mono- and polyubiquitination of the peroxisomal targeting signal co-receptor, Pex20, J. Biol. Chem. 288 (2013) 7230–7240.
[44] D. Hagstrom, C. Ma, S. Guha-Polley, S. Subramani, The unique degradation pathway of the PTS2 receptor, Pex7, is dependent on the PTS receptor/coreceptor, Pex5 and Pex20, Mol. Biol. Cell 25 (2014) 2634–2643.
[45] R. Pan, J. Satkovich, J. Hu, E3 ubiquitin ligase SP1 regulates peroxisome biogenesis in *Arabidopsis*, Proc. Natl. Acad. Sci. U. S. A. 113 (2016) E7307–E7316.
[46] Q. Ling, W. Huang, A. Baldwin, P. Jarvis, Chloroplast biogenesis is regulated by direct action of the ubiquitin–proteasome system, Science 338 (2012) 655–659.
[47] Q. Ling, N. Li, P. Jarvis, Chloroplast ubiquitin E3 ligase SP1: does it really function in peroxisomes? Plant Physiol. 175 (2017) 586–588.
[48] R. Pan, J. Hu, The *Arabidopsis* E3 ubiquitin ligase SP1 targets to chloroplasts, peroxisomes, and mitochondria, Plant Physiol. 176 (2018) 480–482.
[49] M.H. Smith, H.L. Ploegh, J.S. Weissman, Road to ruin: targeting proteins for degradation in the endoplasmic reticulum, Science 334 (2011) 1086–1090.
[50] H.W. Platta, F. El Magraoui, B.E. Baumer, D. Schlee, W. Girzalsky, R. Erdmann, Pex2 and pex12 function as protein-ubiquitin ligases in peroxisomal protein import, Mol. Cell. Biol. 29 (2009) 5505–5516.
[51] F. El Magraoui, R. Brinkmeier, A. Schrotter, W. Girzalsky, T. Muller, K. Marcus, H.E. Meyer, R. Erdmann, H.W. Platta, Distinct ubiquitination cascades act on the peroxisomal targeting signal type 2 co-receptor Pex18p, Traffic 14 (2013) 1290–1301.
[52] M.J. Lingard, M. Monroe-Augustus, B. Bartel, Peroxisome-associated matrix protein degradation in *Arabidopsis*, Proc. Natl. Acad. Sci. U. S. A. 106 (2009) 4561–4566.
[53] C. Williams, M. van den Berg, S. Panjikar, W.A. Stanley, B. Distel, M. Wilmanns, Insights into ubiquitin-conjugating enzyme/co-activator interactions from the structure of the Pex4p:Pex22p complex, EMBO J. 31 (2012) 391–402.
[54] M.R. Groves, C.F.E. Schroer, A.J. Middleton, S. Lunev, N. Danda, A.M. Ali, S.J. Marrink, C. Williams, Structural insights into K48-linked ubiquitin chain formation by the Pex4p–Pex22p complex, Biochem. Biophys. Res. Commun. 496 (2018) 562–567.
[55] K.N. Faber, P. Haima, W. Harder, M. Veenhuis, G. Ab, Highly-efficient electrotransformation of the yeast *Hansenula polymorpha*, Curr. Genet. 25 (1994) 305–310.
[56] M.N. Cepinska, M. Veenhuis, I.J. van der Klei, S. Nagotu, Peroxisome fission is associated with reorganization of specific membrane proteins, Traffic 12 (2011) 925–937.
[57] R.J. Baerends, K.N. Faber, A.M. Kram, J.A. Kiel, I.J. van der Klei, M. Veenhuis, A stretch of positively charged amino acids at the N terminus of *Hansenula polymorpha* Pex3p is involved in incorporation of the protein into the peroxisomal membrane, J. Biol. Chem. 275 (2000) 9986–9995.
[58] M. Komori, S.W. Rasmussen, J.A. Kiel, R.J. Baerends, J.M. Cregg, I.J. van der Klei, M. Veenhuis, The Hansenula polymorpha *PEX14* gene encodes a novel peroxisomal membrane protein essential for peroxisome biogenesis, EMBO J. 16 (1997) 44–53.
[59] P.Z. Ozimek, S.H. Klompmaker, N. Visser, M. Veenhuis, I.J. van der Klei, The transcarboxylase domain of pyruvate carboxylase is essential for assembly of the peroxisomal flavoenzyme alcohol oxidase, FEMS Yeast Res. 7 (2007) 1082–1092.
[60] H.R. Waterham, V.I. Titorenko, P. Haima, J.M. Cregg, W. Harder, M. Veenhuis, The *Hansenula polymorpha* PER1 gene is essential for peroxisome biogenesis and encodes a peroxisomal matrix protein with both carboxy- and amino-terminal targeting signals, J. Cell Biol. 127 (1994) 737–749.
[61] M.D. Abramoff, P.J. Magelhaes, S.J. Ram, Image processing with ImageJ, Biophoton. Int. 11 (2004) 36–42.